Perivascular signals alter global genomic profile of glioblastoma and response to temozolomide in a gelatin hydrogel

Mai T. Ngo[1], Brendan A.C. Harley[2]

[1] Dept. Chemical and Biomolecular Engineering
[2] Carl R. Woese Institute for Genomic Biology
University of Illinois at Urbana-Champaign
Urbana, IL 61801

Corresponding Author:
B.A.C. Harley
Dept. of Chemical and Biomolecular Engineering
Carl R. Woese Institute for Genomic Biology
University of Illinois at Urbana-Champaign
110 Roger Adams Laboratory
600 S. Mathews Ave.
Urbana, IL 61801
Phone: (217) 244-7112
Fax: (217) 333-5052
e-mail: bharley@illinois.edu

ABSTRACT

Glioblastoma (GBM) is the most common primary malignant brain tumor, with patients exhibiting poor survival (median survival time: 15 months). Difficulties in treating GBM include not only the inability to resect the diffusively-invading tumor cells but also therapeutic resistance. The perivascular niche within the GBM tumor microenvironment contributes significantly to tumor cell invasion, cancer stem cell maintenance, and has been shown to protect tumor cells from radiation and chemotherapy. In this study, we describe the development of an *in vitro* artificial perivascular niche (PVN), culturing endothelial and stromal cells along with GBM cells within a methacrylamide-functionalized gelatin hydrogel, in order to examine howthe presence of the PVN alters global genomic expression profiles. Using RNA-seq, we demonstrate that the inclusion of perivascular niche cells with GBM cells upregulates genes related to angiogenesis and remodeling, while downregulated genes are related to cell cycle and DNA damage repair. Signaling pathways and genes commonly implicated in GBM malignancy, such as *MGMT, EGFR*, PI3K-Akt signaling, and Ras/MAPK signaling are also upregulated in the presence of perivascular niche cells. We describe the kinetics of gene expression within the PVN hydrogels over a course of 14 days, observing the patterns associated with previously-observed GBM-mediated endothelial network co-option and regression that are altered in the presence of covalently-bound hyaluronic acid. We finally examine the effect of PVN culture on GBM cell responsiveness to temozolomide, a frontline chemotherapy used clinically against GBM. Notably, the presence of a PVN leads to significantly increased TMZ resistance compared to hydrogels containing only GBM cells. Overall, these results demonstrate that inclusion of cellular and matrix-associated elements of the PVN within *in vitro* models of GBM provide critical signals to regulate the phenotype and therapeutic responsiveness of GBM cells.

Keywords: glioblastoma, hydrogel, perivascular niche, drug response

1. Introduction

Glioblastoma (GBM) is the most common primary malignant brain tumor. Prognosis is grim for GBM patients, with a median survival time of approximately 15 months [1]. Unlike many solid tumors where mortality is linked to metastasis [2], GBM tumors rarely metastasize. Instead, GBM spreads diffusively through the brain by invading along structural elements such as white matter tracts and blood vessels [3-6].Treatment is complicated by the diffuse spreading of tumor cells throughout the brain parenchyma. Poorly-defined tumor margins therefore limit the effectiveness of surgical resection, with tumor cells inevitably left behind after debulking. Subsequent radiation and chemotherapy have limited effect on the remaining tumor cells, with GBM tumors rapidly recurring (median: 6.9mo post debulking) at a site often in close proximity (>90% within 2cm) of the original resection cavity [1, 7]. The need for improved treatment methods for GBM highlights the importance of developing tools to facilitate the understanding of mechanisms of GBM invasion, the role played by interactions between GBM cells and the heterogeneous cell and matrix environment in the surrounding parenchyma, as well as to facilitate drug development and screening.

The heterogeneity of the GBM microenvironment presents a challenge in dissecting the biophysical, biochemical, and cellular cues that drive GBM invasion. In particular, the microenvironment hosts a variety of cell types, including astrocytes, microglia, neural stem cells, pericytes, and endothelial cells, whose interactions with GBM cells have been demonstrated to contribute to heightened invasion potential [8]. Endothelial cells and stromal cells such as pericytes and fibroblast are components of the perivascular niche, in which interactions between blood vessels and GBM cells have been implicated in a variety of roles that promote GBM progression [8, 9]. Tumor cells have been shown to associate closely with blood vessels through co-option as they invade into the surrounding brain parenchyma [4, 10, 11]. Co-opted vessels ultimately undergo regression, triggering hypoxic signaling (HIF-1) in the surrounding

tumor tissue [12-16]. Subsequent secretion of pro-angiogenic factors such as VEGF induces sprouting angiogenesis at the tumor periphery [12, 15]. GBM cells migrates towards these newly-formed blood vessels, thereby pushing the invasive front of the tumor further into the brain parenchyma. Additionally, the perivascular niche potentially contributes to maintenance of cancer stem cells, a highly-resistant subpopulation of cells implicated in tumor recurrence [9, 17, 18]. Crosstalk between endothelial and cancer stem cells may be governed by Notch signaling, which would promote angiogenic activity and stem cell maintenance [8, 9, 17]. The already-demonstrated roles of perivascular cells in promoting GBM invasion warrants further investigation into mechanisms governing endothelial-GBM cell interactions, inhibitors of this cross-talk, and how the interactions between these cell types mediates therapeutic response.

Investigating the interactions between multiple cell types traditionally utilizes conditioned medium in 2D cell culture or migration assays (e.g. Transwell ®), as well as immunofluorescent or immunohistochemical staining and imaging [4, 19, 20]. However, the inability of 2D culture to accurately predict therapeutic response and the complexity of animal models has paved the way for the development of 3D *in vitro* models, which utilize materials such as hydrogels to recapitulate elements of the tumor microenvironment [21-23]. To date, 3D *in vitro* models for GBM primarily incorporate only tumor cells, despite the demonstrated contributions of additional cell types to *in vivo* GBM behavior [6, 24-30]. A few studies have examined the interactions between GBM cells, perivascular niche cells, and macrophages within 3D *in vitro* platforms, but these models feature spatial segregation between the different cell types that is not reminiscent of the *in vivo* microenvironment [20, 31-34]. Mixed cultures of tumor cells, endothelial cells, and stromal cells have been achieved within biomaterials for breast, lung, and prostate cancers, and these models have been used to investigate how non-tumor cells impact tumor proliferation, phenotype, and therapeutic response [35-39]. Our lab has recently described a tri-culture biomaterial platform for the purpose of modeling the perivascular niche of GBM [40]. We

demonstrated the formation of endothelial cell networks in gelatin hydrogels by co-culturing endothelial cells and fibroblasts. Tri-culturing GBM cells alongside these perivascular cells resulted initially in close association between GBM cells and developing endothelial cell networks, followed by dissolution of these networks in a manner similar to vessel co-option and regression *in vivo*. Since hyaluronic acid is an important component of the GBM tumor microenvironment [41], we additionally investigated the effect of matrix-bound hyaluronic acid on endothelial network formation and regression. In this study, we investigated how the presence of a perivascular niche established by endothelial cells and fibroblasts alongside GBM cells alters the global genomic profile of our *in vitro* model within a three-dimensional gelatin hydrogel. We use RNA sequencing (RNA-seq) to determine differentially-expressed genes resulting from tri-culturing perivascular cells with GBM cells, comparing results to cultures of GBM cells alone and perivascular cells cultured in the absence of tumor cells. Additionally, we traced the expression of select genes commonly implicated in GBM malignancy (e.g. *VEGF*, *HIF1α*, *MMP9*, *TNC*, *EGFR*) as a function of time and the presence of hydrogel immobilized hyaluronic acid content. We further investigated how the presence of perivascular niche established by culture with endothelial and stromal cells acts as a protectant against GBM cell response to temozolomide (TMZ), the frontline alkylating agent used clinically to treat GBM.

2. Materials and Methods

2.1. Cell Culture

Human umbilical vein endothelial cells (HUVECs) and normal human lung fibroblasts (NHLF) were purchased from Lonza (Walkersville, MD) and used before passage 6 and passage 8 respectively. HUVECs were cultured in EGM-2 media containing 2% FBS and supplements such as hEGF, hydrocortisone, VEGF, hFGF-B, R^3-IGF-1, ascorbic acid, heparin, and gentamicin/amphotericin-B (Lonza, Walkersville, MD) [42]. NHLFs were cultured in FGM-2 media containing 2% FBS and supplements such as hFGF-B, insulin, and

gentamicin/amphotericin-B (Lonza, Walkersville, MD) [2]. U87-MG cells, a gift from Professor Nathan D. Price (ISB, Seattle), were cultured in DMEM with 10% FBS and 1% penicillin/streptomycin [28]. All cell types were cultured at 37 °C in 5% CO_2.

2.2. Fabrication of cell seeded gelatin hydrogels

Two distinct hydrogel formulations were used throughout all experiments. Both hydrogel variants were based on a methacrylamide-functionalized gelatin (GelMA) macromer previously developed in our lab for culture of GBM cells [27] [28]. GelMA and HAMA were synthesized as previously described, and the degree of functionalization of GelMA was determined to be 50% by ^{1}H NMR [28]. GelMA alone or GelMA combined with 15% w/w HAMA (GelMA + HA) were dissolved in PBS at 65 °C to form 4 wt% polymer solutions. Lithium acylphosphinate (LAP) was added as a photoinitiator at 0.1% w/v for GelMA-only gels and 0.02% w/v for GelMA/HAMA gels. The reduced photoinitiator concentration allowed for equivalent elastic moduli (~3 kPa) between the GelMA and GelMA + HA constructs [40]. Cell seeded hydrogels (GelMA only; GelMA+HA) were then formed in one of three configurations: *GBM-only*; *Perivascular-only*; or *Tri-Culture*. *GBM-only* cultures were formed by re-suspending 1×10^5 U87-MGs/mL in the GelMA or GelMA+HA polymer solution. *Perivascular-only* cultures were formed by re-suspending 1×10^6 HUVECs/mL and 2×10^6 NHLFs/mL in the GelMA or GelMA+HA polymer solution. *Tri-Cultures* were formed by re-suspending 1×10^6 HUVECs/mL, 2×10^6 NHLFs/mL, and 1×10^5 U87-MGs/mL in the GelMA or GelMA+HA polymer solution. Cell-laden solutions were subsequently pipetted into circular Teflon molds with a diameter of 5 mm and a thickness of 1 mm, and exposed to UV light at a wavelength of 365 nm and intensity of 5.69 mW/cm^2 for 30 s as previously described to form cell-seeded hydrogel disks [40]. Hydrogels were maintained for up to 14 days in 48-well plates in EGM-2 media with daily media changes.

2.3. Flow cytometric analysis of GBM and perivascular populations

Perivascular-only cultures (endothelial and stromal cells) and *Tri-Cultures* (GBM, endothelial, and stromal cells) were dissociated using a protocol adapted from *van Beijnum et al.* [43] at 3, 7, and 14 days post-culture. Briefly, cell-seeded hydrogels were dissociated in a solution of collagenase type IV (230 U/mL, Worthington, Lakewood, NJ), dispase (0.23 U/mL, Thermo Fisher Scientific, Waltham, MA), and hyaluronidase (8 U/mL, Sigma Aldrich, St. Louis, MO). The resulting cell solution was filtered through a 100 μm cell strainer (Thermo Fisher Scientific, Waltham, MA), centrifuged, and re-suspended in PBS with 0.1% sodium azide (Sigma Aldrich, St. Louis, MO), 1% penicillin/streptomycin, and 2% FBS. Cells were stained with Alexa Fluor 488-conjugated CD90 (5:100, R&D Systems, Minneapolis, MN; NHLFs) and propidium iodide (PI, 1:1000, Thermo Fisher Scientific, Waltham, MA; Dead cells). Flow cytometry was then performed using a BD LSR II flow cytometer (BD Biosciences, San Jose, CA). Data was subsequently analyzed using FCS Express 6.0 software (De Novo Software, Glendale, CA), first gating for cells (FSC-A/SSC-A), then viability through PI exclusion, then Alexa Fluor 488 fluorescence to determine the CD90+ fraction of each sample.

2.4. RNA Isolation and Quality Analysis

Hydrogels were collected at 0, 3, 7, and 14 days and stored at -80 °C until RNA extraction. RNA was extracted using an RNeasy Plant Mini Kit, followed by DNase digestion using a RNase-free DNase set (Qiagen, Hilden, Germany) [44]. RNA samples for RNA-seq were analyzed for quality using an Agilent 2100 bioanalyzer (Agilent, Santa Clara, CA). Samples with a minimum RIN of 7 were used for RNA-seq [45]. Quality testing of RNA was performed by the Roy J. Carver Biotechnology Center at the University of Illinois Urbana-Champaign.

2.5. RNA-seq analysis of Tri-Culture hydrogels

RNA-seq was performed on RNA samples from the *Tri-Culture* hydrogels (GBM, endothelial, and stromal cells), as well as RNA samples comprised of a mixture of RNA from the

Perivascular-only and *GBM-only* culture conditions (*Mixed*). The comparison between *Tri-Culture* and *Mixed* samples was inspired by the methodology described by *Lilly et al.* [46]. *Mixed* samples were constructed such that the CD90+ fraction of the *Tri-Culture* and *Mixed* samples were equal. Libraries for RNA sequencing were prepared using the TruSeq Stranded mRNAseq Sample Prep Kit (Illumina, San Diego, CA), which fragments the mRNA, reverse transcribes it to cDNA, and adds sequence adaptors [47]. Libraries were subsequently quantitated with qPCR and sequenced by using the HiSeq 4000 sequencing kit version one in conjunction with a HiSeq 4000 (Illumina, San Diego, CA). 100 nt single-end reads were generated in 101 cycles to yield 55 – 70 million reads per sample. Library preparation and sequencing were performed by the Roy J. Carver Biotechnology Center at the University of Illinois Urbana-Champaign.

Library quality was checked using FastQC, and Trimmomatic [48] was used to remove low-quality reads. Trimmed libraries were subsequently aligned to the human genome (GRCh38.p10) using STAR [49], and featureCounts [50] was used to categorize the aligned reads to genes and other genomic features. 45393 genes were identified from the reads. Differential gene expression analysis was performed in R using limma and edgeR packages [51] [52]. Quality control was performed to filter out genes with few counts using a threshold of 0.5 counts per million, with 14269 genes remaining after applying the threshold. This accounted for >99% of the counts and 31% of the identified genes. TMM normalization was performed before determining differentially expressed genes. Functional annotation was performed, followed by gene ontology (GO) and KEGG pathway analyses using GOstats [53].

2.6. Real-time PCR

RNA was reverse transcribed to cDNA using reagents from the QuantiTect Reverse Transcription Kit (Qiagen, Hilden, Germany) and a Bio-Rad MyCycler thermal cycler (Bio-Rad, Hercules, CA). Real-time PCR was performed in an Applied Biosystems QuantStudio 7 Flex

PCR System (Thermo Fisher Scientific, Waltham, MA) using Taqman Fast Advanced Master Mix and Taqman Gene Expression Assays (Thermo Fisher Scientific, Waltham, MA) (**Table 1**). RPS20 was used as the housekeeping gene [54]. Fold change was calculated using the $\Delta\Delta C_T$ method and normalized to expression at Day 0 in hydrogels without HAMA [55].

2.7. Analysis of GBM response to Temozolomide (TMZ)

Tri-culture and *GBM-only* hydrogels were developed with and without HAMA and cultured for 7 days in EGM-2 media with daily media change. After 7 days of culture, TMZ (Sigma Aldrich, St. Louis, MO) was added at 0, 100, 250, and 500 μM to all hydrogels for 48 hours. To assess cellular response to TMZ, metabolic activity was assessed using a 3-(4,5-dimethylthiazol-2-yl)-2,5-diphenyltetrazolium bromide (MTT) assay (Thermo Fisher Scientific, Waltham, MA) 48 hours after treatment [56]. Hydrogels were incubated in 200 μL EGM-2 media and 20 μL MTT solution for 4 hours at 37 °C. The resultant formazan was solubilized into 300 μL DMSO (Sigma Aldrich, St. Louis, MO) overnight. Absorbance was read at 540 nm using a BioTek Synergy HT microplate reader (BioTek, Winooski, VT). Metabolic activity for treated samples was normalized to the untreated control. Additionally, growth rate inhibition (GR), as described in *Hafner et al.* [57], was measured in hydrogels at concentrations of 0, 25, 100, 250, and 500 μM TMZ after 7 days of culture. Relative cell count was assessed after 48 hours after treatment with the CellTiter-Glo Luminescent Cell Viability assay (Promega, Madison, WI) using a protocol derived from *Lin et al.* [58]. Briefly, hydrogels were incubated for one hour at room temperature in 150 μL EGM-2 media mixed with 150 μL CellTiter reagent. Luminescence was read using a BioTek Synergy HT microplate reader. Initial cell counts were obtained by running the assay on untreated hydrogels on the day of treatment. GR metrics were calculated as described by *Hafner et al.* [57], and the GR_{50} was calculated using the Online GR Calculator

(www.grcalculator.org/grcalculator). DMSO at the highest relative concentration was used as the untreated control (0 μM).

2.8. Statistics

Statistical analysis for real-time PCR and drug treatment experiments was performed using one-way ANOVA followed by Tukey post hoc in OriginPro (OriginLab, Northampton, MA). Differential gene expression, gene ontology, and KEGG pathway analyses were performed in R as previously described. All experiments used n = 3 hydrogels per group. Significance was set at $p < 0.05$ for all analyses except for differential gene expression, in which an FDR adjusted p-value < 0.05 was used. Data are presented as mean ± SD.

3. Results

3.1. Presence of perivascular niche cells alters genomic profile of glioblastoma within gelatin hydrogels

We used RNA-seq to analyze the genomic profile of *Tri-Culture* GelMA-only hydrogels in contrast with *Perivascular-only* and *GBM-only* GelMA-only hydrogels. RNA from the *Tri-Culture*

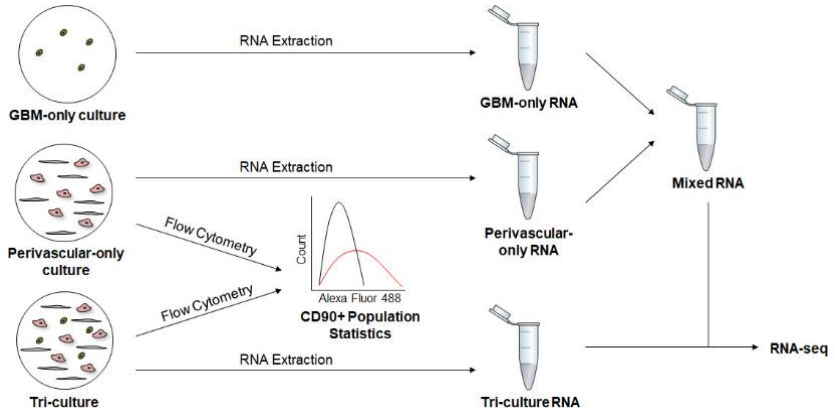

Figure 1. Schematic of workflow for preparing RNA samples for RNA-seq. RNA was extracted from *GBM-only*, *Perivascular-only*, and *Tri-Culture* hydrogels. Flow cytometry was performed on cells from additional *Perivascular-only* and *Tri-Culture* hydrogels to obtain the fraction of $CD90^+$ cells in each culture system. *GBM-only* and *Perivascular-only* RNA were subsequently combined to form a *Mixed* sample such that the $CD90^+$ fraction of the *Mixed* sample was equal to that in the *Tri-Culture* sample. *Mixed* and *Tri-Culture* RNA were subsequently sequenced.

hydrogels (*Tri-Culture*) was compared to RNA samples (*Mixed*) constructed from combining RNA from separate *Perivascular-only* and *GBM-only* hydrogels (**Figure 1**), such that the CD90+ fraction (NHLF sub-population) of the mixed samples would match that in the *Tri-Culture* samples (**Table 2**). Differential gene expression analysis identified 1737 significantly upregulated genes (FDR-adjusted $p < 0.05$) and 1778 significantly downregulated genes (FDR-adjusted $p < 0.05$) in the *Tri-Culture* compared to the *Mixed* samples (**Figure 2, Supplementary Tables 1-2**). Samples clustered together based on whether they were *Tri-Culture* or *Mixed* samples (**Figure 2**). Significantly upregulated genes included several related to angiogenesis (e.g. *FGFR1*, *FLT1*, *TEK*, *VEGFB, RUNX1*), PDGF signaling (e.g. *PDGFB*, *PDGFRA*, *PDGFRB*), Notch signaling (e.g. *Notch1*, *Notch2*, *Notch3*, *Notch4*, *DLL4*), extracellular matrix proteins (e.g. *CSPG4*, *TNC*, *FN1*), extracellular matrix remodeling (e.g. *MMP1*, *MMP8*, *MMP9*, *MMP12*, *MMP14*, *MMP19*), stromal activation (e.g. *FAP*), hyaluronic acid (e.g. *HAS2*, *CEMIP*), as well as multiple genes previously shown to be over-expressed in GBM (e.g. *CTSK*, *EGFR*, *JUN*, *MGMT*, *GFPT2*) [59-62] (**Supplementary Table 1)**. Downregulated genes also included those related to hyaluronic acid production and binding (e.g. *HAS1, HMMR*), proliferation (e.g.

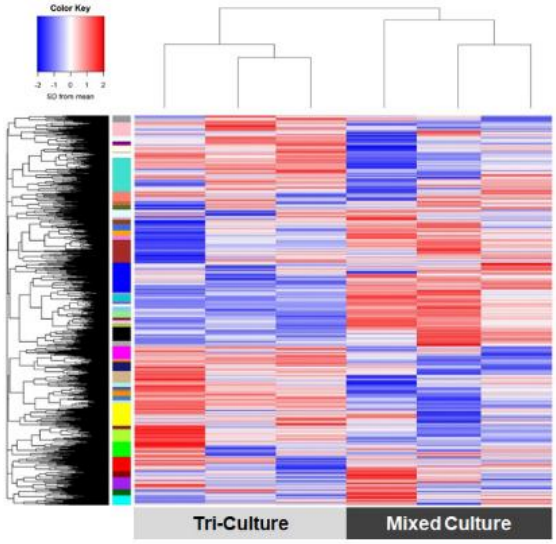

Figure 2. Expression pattern of genes detected during RNA-seq of *Tri-Culture* and *Mixed* samples. Color Key: SD from mean of log(Counts per Million) scaled such that values are centered at 0. N = 3.

MKI67), cell cycle (e.g. *CDKN2B*, *RBL1*, *BUB1*, *BUB1B*), and DNA damage repair (e.g. *MSH2*, *MSH6*, *MLH1*) (**Supplementary Table 2)**.

We subsequently used Gene Ontology (GO) analysis to identify over-represented terms amongst upregulated and downregulated genes. Specifically, over-represented GO terms amongst upregulated genes included those related to response to stimulus, signaling, development, cell motility, secretion, regulation of cell death, adhesion, neurogenesis, vascular development and angiogenesis, hypoxia, ECM organization, and fibroblast activation (**Supplementary Table 3**). Within downregulated genes, terms related to RNA processing and stability, DNA damage detection and response, response to oxidative stress, double-strand break repair, and postreplication repair were over-represented (**Supplementary Table 4**). Additionally, terms related to metabolism, biosynthesis, cell cycle and proliferation regulation, base excision repair, and regulation of gene expression, transcription, and silencing were over-represented amongst both upregulated and downregulated genes.

KEGG pathway analysis revealed various signaling cascades, including Notch, MAPK, and HIF-1 were over-represented amongst upregulated genes (**Figure 3a**). Additional over-represented

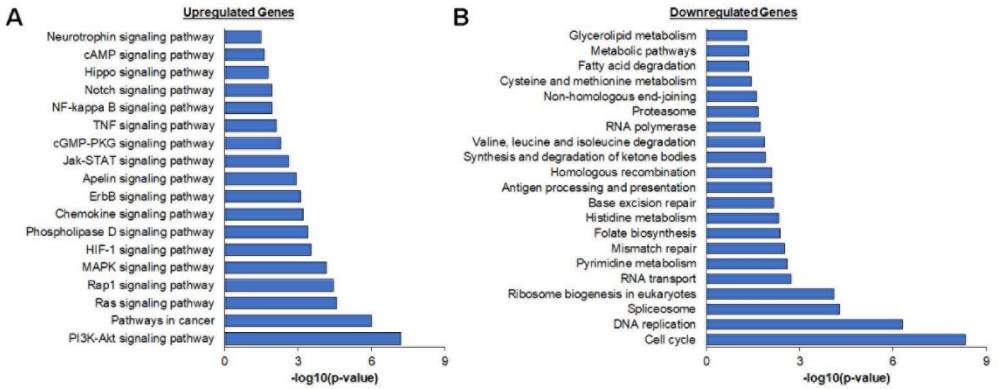

Figure 3. KEGG pathway analysis on significantly upregulated and downregulated genes. **(A)** Various pathways commonly dysregulated in cancer were over-represented amongst upregulated genes. **(B)** Pathways related to metabolism, DNA repair, and cell cycle were over-represented amongst downregulated genes.

terms included glycosaminoglycan biosynthesis, cellular senescence, cell adhesion molecules, transcriptional misregulation in cancer, starch and sucrose metabolism, EGFR tyrosine kinase inhibitor resistance, regulation of actin cytoskeleton, glioma, proteoglycans in cancer, focal adhesion, and interactions between cytokine-cytokine receptor and ECM-receptor (**Supplementary Table 5**). Notably, over-represented amongst downregulated genes were terms related to metabolism, biosynthesis and degradation, cell cycle, DNA replication, and various DNA damage repair mechanisms (**Figure 3b, Supplementary Table 6**).

3.2. Malignancy-related genes vary temporally in tri-culture hydrogels

We subsequently used real-time PCR to investigate the kinetics of gene expression in *Tri-Culture* hydrogels over a period of 14 days (**Figures 4** - **6**). We examined a panel of genes related to angiogenesis (i.e. *VEGF, VEGFR1, ANG1, ANG2, TIE2*), hyaluronic acid synthesis and signaling (i.e. *RHAMM*, *HAS1*, *HAS2*), re-modeling (i.e. *MMP9*), PDBF signaling (i.e. *PDGFB, PDGFRA, PDBFRB*), hypoxia (i.e. *HIF1α*), proliferation (i.e. *KI67*), stromal cross-talk (i.e. *FAP*), as well as *TNC* and *EGFR*, which have been previously implicated in GBM progression in literature [54] [61]. These genes were chosen from those that were identified as significantly upregulated or downregulated in the RNA-seq analysis, or from those implicated in

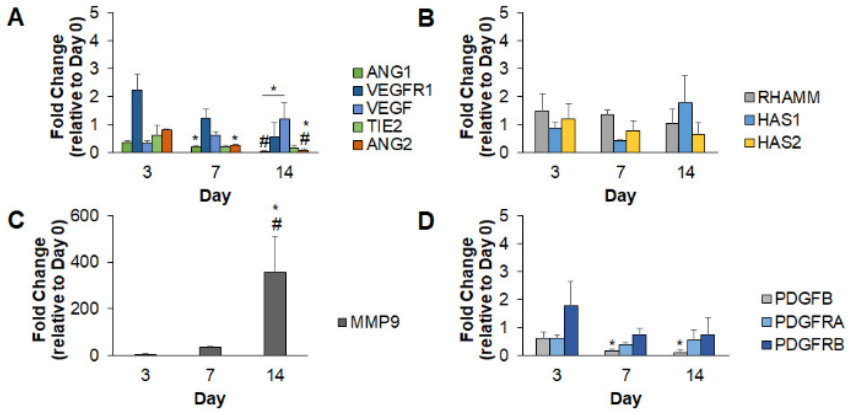

Figure 4. Gene expression profiles for GelMA-only *Tri-Culture* hydrogels over the course of 14 days. Genes studied were related to **(A)** angiogenesis, **(B)** hyaluronic acid sensing and synthesis, **(C)** tissue remodeling, and **(D)** PDGF signaling. *p<0.05 compared to Day 3. #p<0.05 compared to Day 7. Data is presented as mean ± SD. N = 3.

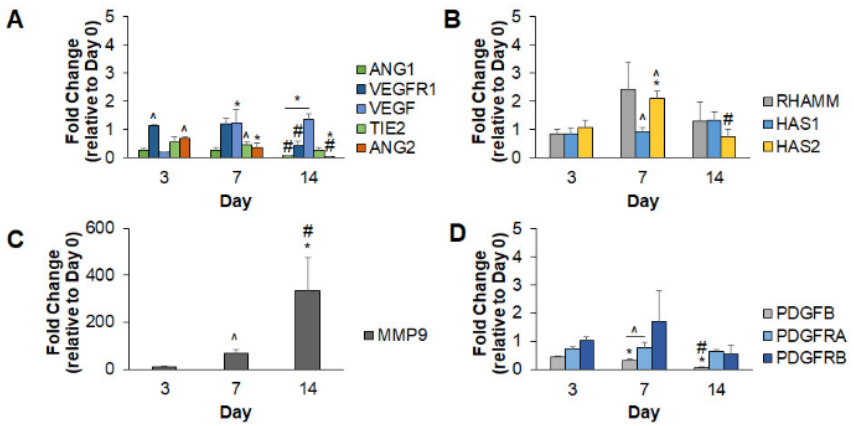

Figure 5. Gene expression profiles for *Tri-Culture* hydrogels containing brain-mimetic immobilized hyaluronic acid (GelMA+HAMA) over the course of 14 days. Genes studied were related to **(A)** angiogenesis, **(B)** hyaluronic acid sensing and synthesis, **(C)** tissue remodeling, and **(D)** PDGF signaling. *p<0.05 compared to Day 3. #p<0.05 compared to Day 7. ^p<0.05 compared to GelMA-only hydrogels (**Figure 4**) at same timepoint. Data is presented as mean ± SD. N = 3.

prior literature regarding GBM invasion and vascularization [63] [64]. Notably, within angiogenesis-related genes, *ANG1* and *ANG2* expression significantly decreased over 14 days, and *TIE2* expression additionally trended downwards from Day 3 to Day 7 in GelMA hydrogels (**Figure 4a**). *VEGFR1* expression was significantly downregulated, while *VEGF* was significantly upregulated by Day 14 compared to Day 3. Within genes related to hyaluronic acid synthesis and signaling, *RHAMM, HAS1*, and *HAS2* were expressed during the culture period, but no significant trends were observed (**Figure 4b**). With regards to tissue remodeling, *MMP9* expression significantly increased by Day 14 compared to Days 3 and 7 (**Figure 4c**). Within PDGF signaling, *PDGFB* expression significantly decreased with time, while *PDGFRB* trended downwards with time (**Figure 4d**). *FAP* expression, which relates to stromal activation, was significantly downregulated by Day 14 (**Figure 6a**). *HIF1α* expression trended downwards with time, while *TNC* expression trended upwards.

3.3 Presence of covalently-bound hyaluronic acid within the hydrogels alters gene expression profiles

We additionally investigated the kinetics of *Tri-Culture* gene expression patterns in HA-functionalized GelMA hydrogels. For genes related to angiogenesis, trends were similar to those observed in the absence of HAMA (**Figure 5a**). However, *VEGR1* and *ANG2* were downregulated with the presence of HAMA at Day 3, while *TIE2* was upregulated at Day 7 compared to cultures without HAMA. In contrast to cultures without HAMA, in which both *RHAMM* and *HAS2* trended downwards with time, expression in cultures with HAMA trended towards a peak at Day 7 (**Figure 5b**). Hyaluronic acid synthase genes *HAS1* and *HAS2* were significantly upregulated at Day 7 with the presence of HAMA while the gelatinase *MMP9* was significantly upregulated with time, with further increased expression at Day 7 in the presence of matrix-bound HA (**Figure 5c**). Additionally, *PDGFB* and *PDGFRA* were upregulated at Day 7 in hydrogels with covalently-bound HA (**Figure 5d**). In contrast to GelMA-only cultures, *PDGFRB* trended towards a peak at Day 7 instead of Day 3 (**Figure 5e**). Trends in *FAP* and *TNC* expression were not altered by HAMA (**Figure 6b**). While *HIF1α* remained relatively constant with time, *KI67* and *EGFR* expression both appeared to peak at Day 7.

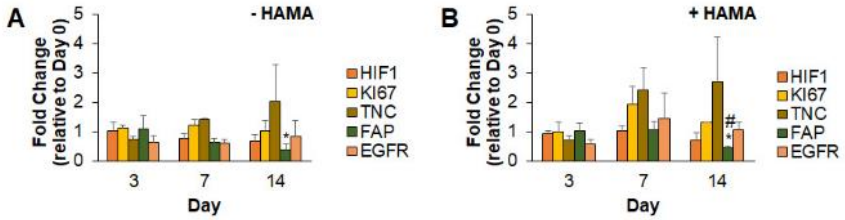

Figure 6. Gene expression profiles for various genes related to GBM malignancy in **(A)** GelMA-only and **(B)** GelMA+HAMA *Tri-Culture* hydrogels. *p<0.05 compared to Day 3. #p<0.05 compared to Day 7. Data is presented as mean ± SD. N = 3.

3.4 Tri-culture and GBM-only hydrogels differentially respond to TMZ

The comparison of *Tri-culture* hydrogels to *Perivascular-only* and *GBM-only* hydrogels using RNA-seq revealed significant upregulation of *MGMT* and significant downregulation of genes associated with DNA mismatch repair, which has been implicated in resistance to TMZ, the standard chemotherapy for GBM [65]. As such, we hypothesized that *Tri-culture* hydrogels would demonstrate increased resistance to TMZ compared to *GBM-only* hydrogels. GBM cells

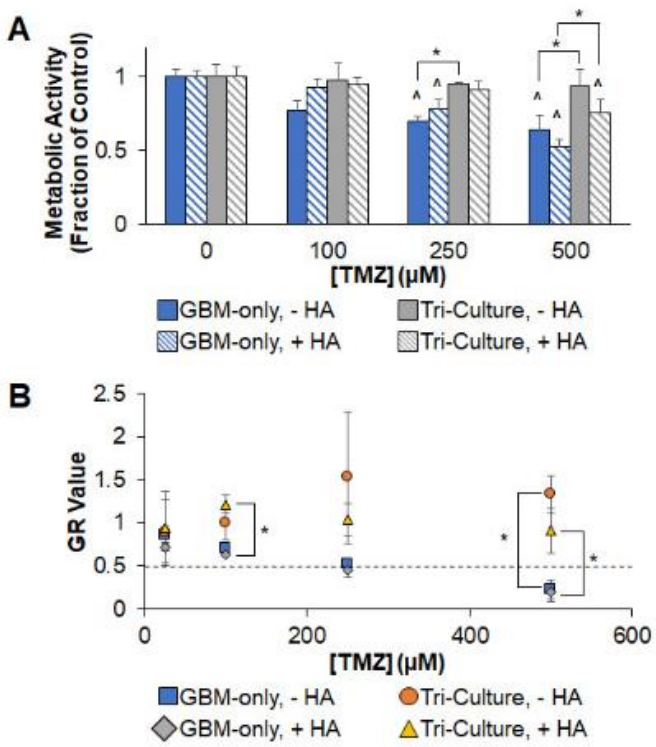

Figure 7. Comparison of response to TMZ in *GBM-only* and *Tri-Culture* hydrogels. **(A)** Metabolic activity (measured by MTT assay) was significantly reduced in *GBM-only* cultures (higher response to TMZ) compared to *Tri-Cultures* after treatment with 250 µM and 500 µM TMZ. ^p<0.05 compared to untreated control. *p<0.05 between groups. **(B)** Growth rate (GR) inhibition occurred in *GBM-only* hydrogels with increasing concentrations of TMZ, but was not observed in *Tri-Culture* hydrogels. *p<0.05 between groups. Data is presented as mean ± SD. N = 3.

were allowed to stabilize in GelMA and GelMA+HA hydrogels for seven days before treatment to allow the establishment of a perivascular niche-like environment within the *Tri-Culture* hydrogels. We analyzed response to TMZ 48 hours after treatment by assessing changes in metabolic activity and growth rate inhibition. In response to TMZ treatment the metabolic activity of GBM cells in GelMA hydrogels decreased significantly (250 µM, 500 µM TMZ) compared to untreated controls for *GBM-only* cultures (**Figure 7a**). The presence of matrix-immobilized HA did not significantly alter the reduction in metabolic activity in *GBM-only* cultures. Interesting, *Tri-Culture* hydrogels that contained a perivascular culture did not exhibit significant decreases in metabolic activity until application of 500 µM TMZ, and there only for HA-modified GelMA hydrogels. Metabolic activity trended downwards for *Tri-Culture* hydrogels in GelMA only hydrogels but was never significantly diminished over the range of tested TMZ concentrations.

We additionally used a cell-viability assay to measure growth rate inhibition in *GBM-only* and *Tri-Culture* hydrogels in response to TMZ treatment (**Figure 7b**). In corroboration with trends observed in metabolic activity, we did not observe growth rate inhibition in *Tri-Culture* hydrogels across the concentrations tested. In contrast, growth rate (GR) values decreased with increasing TMZ concentrations in *GBM-only* hydrogels. Using the Online GR Calculator, we estimated GR_{50} = 232 μM for *GBM-only* GelMA-only hydrogels and GR_{50} = 160 μM for *GBM-only* GelMA+HAMA hydrogels. With 500 μM TMZ treatment, we observed significantly reduced GR values for *GBM-only* cultures versus *Tri-Culture* environments containing a perivascular niche (**Figure 7b**).

4. Discussion

GBM progression is believed to be linked to the interactions of cancer cells with endothelial cells and associated stromal cells within the perivascular niche. Previous efforts have shown GBM invasion into healthy brain parenchyma proceeds along blood vessels, with vessel co-option followed by subsequent regression and angiogenic sprouting at the tumor periphery further expands the tumor margins [11, 12, 15]. The perivascular niche has also been implicated in the maintenance of cancer stem cells, potentially through crosstalk between cancer stem cells and endothelial cells via Notch signaling, and may potentially contribute to GBM resistance to therapy [17, 18, 66, 67]. Previously, predominantly 2D culture or Transwell-based migration assays, as well as *in vivo* animal models, have been traditionally used to study interactions between GBM and endothelial cells [4, 19]. However, 2D and Transwell models may be limited by the lack of a 3D matrix architecture or limited direct cell-cell contact. Animal models are physiologically relevant, but difficulties exist in extracting sufficient quantities of analyzing cell subpopulations [68]. Further, the timescale for in vivo studies can be disadvantageous for

developing real-time and personalized therapeutic regimens. The potential for 3D *in vitro* models of GBM to recapitulate physiologically-relevant phenotype in a timely manner has already been demonstrated through a variety of biomaterials using PEG, collagen, hyaluronic acid, and gelatin chemistries [24, 25, 28]. However, few models have included additional cell types in co-culture with GBM cells [20, 33], suggesting that a 3D *in vitro* model of the GBM perivascular niche may be particularly advantageous given its suggested role in promoting invasion and therapeutic resistance.

We have previously demonstrated that endothelial cell networks can be sustained and tuned within gelatin hydrogels using a co-culture and endothelial cells and fibroblasts [40]. We also observed that including U87-MG GBM cells in the culture system leads to close association between GBM cells and the developing endothelial cell networks, followed by dissolution of these networks in a manner reminiscent of co-option [69]. In this study, we were interested in defining the degree to which the addition of a perivascular niche within the hydrogel culture alters the genomic profile of the *in vitro* model compared to hydrogels containing only GBM cells. We additionally quantified the kinetics of genomic changes that accompanied the development and dissolution of the endothelial cell networks over 14 days of culture *in vitro*. And based on the mechanism of action of the alkylating agent TMZ used currently as a frontline GBM therapy in the clinic as well as result of the global RNA-seq analysis, we examined whether the *in vitro* perivascular niche provided a protective environment against TMZ therapy.

We utilized RNA-seq to determine if the inclusion of perivascular niche cells within the hydrogel model further promoted the recapitulation of characteristics of GBM phenotype compared to culturing GBM cells or perivascular niche cells alone after 7 days of culture. Upregulation of angiogenesis-related genes correlated to *in vitro* observations that GBM cells promote endothelial cell migration and capillary formation, and was also consistent with previous findings

using *in vivo* models and patient samples [20, 33, 63, 70-72]. Differential gene expression analysis also demonstrated upregulation of several genes previously linked to GBM malignancy, such as the matrix metalloproteinases, *PDGFB* and PDGF receptors, *TNC*, *FN1*, and *EGFR*, consistent with previous findings using conventional cell culture and analysis of patient and xenograft-derived tumor specimens [54, 61, 73-75]. KEGG pathway analysis additionally confirmed the over-representation of various signaling cascades commonly dysregulated in GBM amongst upregulated genes, such as Notch, NF-κβ, Jak-STAT, HIF-1, MAPK, Ras, and PI3K-Akt [9] [76] [77] [78], all in the case of GBM cells exposed to a perivascular environment. Notch signaling in particular has been previously associated with the perivascular niche and implicated in cancer stem cell maintenance and angiogenesis associated with poor patient outlook [9, 17]. The results of this analysis suggest that crosstalk between GBM and non-GBM perivascular niche associated cell types within the microenvironment contributes to the overall tumor phenotype.

KEGG pathway and GO analysis revealed that while upregulated genes in the presence of a perivascular environment were commonly associated with cell migration, downregulated genes were linked to cell cycle and proliferation. These results correlate with the “go or grow” hypothesis, which suggests that cells will either migrate or proliferate at a given point in time [79]. The relevance of the “go or grow” hypothesis in GBM has been demonstrated by *Mariani et al.*, who used microarray analysis to show that cell cycle, proliferation, and apoptotic genes were downregulated in migrating GBM cells [80]. Additionally, time-lapse imaging performed by *Farin et al.* demonstrated that while GBM cells invade along blood vessels, these cells would stop migrating in order to proliferate before resuming movement [11]. It has also been shown that endothelial cells within the GBM microenvironment are more migratory and less proliferative than endothelial cells from normal brain tissue, which would further correlate to the results observed in this study [81]. Interestingly, downregulated genes in the *Tri-Culture* (GBM cells in

the presence of a perivascular environment) also included those previously shown to be upregulated in GBM, such as *ADGRG1* and *CD74* [59]. Discrepancies between the results presented here and those from prior literature may be explained by the fact that we compared RNA from the *Tri-Culture* model to RNA from a mixture of tumor and non-tumor cells, as opposed to non-malignant cells or tissue. This comparison was made to contrast between 3D *in vitro* models containing GBM cells alone and GBM cells in culture with perivascular niche cells. Further validation of our *Tri-Culture* model may be achieved by performing differential gene expression analysis against a model of non-malignant brain tissue.

Vessel co-option and regression has been observed to precede sprouting angiogenesis at the tumor margins in GBM [12]. *Holash et al.* described the expression of *ANG2* by co-opted vessels within an *in vivo* model, as well as delayed expression of VEGF after regression occurs [12]. *ANG2* is also expressed by vessels formed as a result of angiogenesis that occurs after regression. Within our tri-culture model, we observed behavior reminiscent of co-option and regression over the course of 14 days. *ANG2* expression was highest at Day 3, when close association was already observed between developing endothelial network structures and U87-MG cells. Since an angiogenic response to regression was not observed within the culture period, *ANG2* expression was not expected at Day 14. On the other hand, maximal *VEGF* expression as observed at Day 14, most likely as a response by the tumor cells to the regressing endothelial network regression. Decreasing expression of *VEGFR1* and *TIE2*, which are both found on endothelial cells, additionally accompanied regression and the associated endothelial cell apoptosis. We also observed decreasing expression of *FAP* and *PDGFRB*, which are both associated with stromal and endothelial cells [63]. This trend may also be linked to the regression of the perivascular compartment of the culture. Interestingly, while *Stratmann et al.* observed that *ANG1* was expressed in tumor cells and *Holash et al.* found that *ANG1* expression did not change with tumor progression, we observed a decline in *ANG1* expression

over the culture period [12, 82]. While this could be explained by apoptosis of the tumor cells, investigation into cell type-specific genomic profile changes will help us resolve the role of *ANG1* within our model.

In addition to profiling of genes implicated in vascular regression and angiogenesis, we analyzed the kinetics of genes commonly implicated in GBM progression via RT-PCR. We observed significant upregulation of *MMP9*, which *Raithatha et al.* showed to be expressed by both tumor cells and vessels *in vivo* [73]. *TNC* expression also increased during the culture period, consistent with observations of *TNC* upregulation in samples from GBM patients with poor prognosis [54]. These trends, as well as constant expression of *EGFR* and *HIF1*, provide evidence that the tri-culture model recapitulates elements of the *in vivo* phenotype of GBM.

Hyaluronic acid (HA) is a major component of the GBM microenvironment, and interactions with between tumor cells and HA through CD44 and other HA receptors impacts GBM phenotype [6, 28, 30, 41, 83]. While gene expression trends for GBM cells in the presence of a perivascular niche were largely conserved in GelMA hydrogels with the presence or absence of matrix-immobilized HA, we observed increased expression of *HAS1* and *HAS2* at Day 7 in HA-decorated hydrogels, consistent with previous findings in our lab regarding GBM invasion mechanisms that also observed that *HAS1* and *HAS2* expression increased in the presence of matrix-bound HAMA [30]. We also observed PDGF signaling was increased at Day 7 in the presence of HAMA, further suggesting that the composition of the microenvironment plays a role in determining GBM behavior.

The ability for 3D *in vitro* models of GBM to accurately recapitulate *in vivo* phenotype presents opportunities for such platforms to be used to investigate drug response in an efficient manner and potentially facilitate drug discovery. The current standard chemotherapy for GBM is

temozolomide (TMZ), and *MGMT expression* as well as the DNA mismatch repair (MMR) pathway are two mechanisms implicated in TMZ resistance [65]. Based on the upregulation of *MGMT* and the downregulation of MMR genes in the *Tri-Culture* as observed via RNA-seq, we hypothesized that the *Tri-Culture* hydrogels would be more resistant to TMZ treatment compared to *GBM-only* hydrogels. We confirmed heightened resistance to TMZ in the tri-culture compared to the GBM-only model using metabolic and cell viability assays. Metabolic activity in the *Tri-Cultures* was essentially unchanged compared to the untreated control across all tested drug concentrations, while metabolic activity declined in the *GBM-only* model at the highest concentrations of TMZ. Additionally, growth rate inhibition was only observed in *GBM-only* hydrogels, with significantly decreased growth metrics in the *GBM-only* hydrogels versus the *Tri-Culture* environment at the highest concentration of TMZ. The differential response to TMZ observed between the two models corroborates with the RNA-seq results. *MGMT* has been implicated in repairing the O^6-methylguanine lesion caused by TMZ action [84], and *MGMT* silencing through promoter methylation is seen in a fraction of GBM patients, who respond more favorably to TMZ treatment compared to patients with functioning *MGMT* [85]. Additionally, functional MMR mechanisms lead to apoptosis after exposure to TMZ, and thus downregulation would lead to resistance [65]. The perivascular niche has been associated with therapeutic resistance, partially due to its ability to maintain a resistant cancer stem cell population [18], however in this study the GBM cell line we employed does not contain a measurable GBM stem cell population (not shown). Studies have suggested that endothelial cells are resistant to TMZ, which would additionally contribute to resistance [86, 87]. Taken together, these results demonstrate that the tri-culture model recapitulates heightened therapeutic resistance associated with the perivascular niche, and represents a promising opportunity for future studies that deduce signaling pathways contributing to resistance and propose potential inhibitors to improve therapeutic response.

Overall, we demonstrate that the inclusion of perivascular niche cells in a 3D *in vitro* model of GBM allows for further recapitulation of elements of *in vivo* phenotype within the model, including resistance to TMZ. We acknowledge that use of this platform is limited by our current approaches in analyzing the global genomic and proteomic profiles of the culture system as a whole. While these results have been informative in determining the overall similarities between this *in vitro* model and native GBM, future work will interrogate genomic and secretome profiles of endothelial and tumor cell subpopulations individually in order to understand specific cell-cell interactions that occur within the perivascular niche to drive GBM malignancy. Techniques such as single-cell RNA-seq and heavy isotope labeling have been used in recent literature to study cell-cell interactions in GBM and other tumor types, and can be used with this tri-culture model [88-90]. Additionally, in order to investigate angiogenic events after vessel regression, we must add spatial resolution to the platform such that tumor cells are invading into an existing endothelial cell network, as opposed to the network developing in the presence of tumor cells. Our lab has developed methods to create spatially-graded hydrogels for the culture of patient-derived GBM biospecimens and to examine therapeutic resistance to EGFR tyrosine kinase inhibitors [29, 91], and could be adapted to generate spatially-graded perivascular models. The transition from GBM cell lines to patient-derived cells provides an opportunity to use this approach to study the behavior of cancer stem cells and their interactions with artificially created perivascular niches within a hydrogel environment. We plan to culture patient-derived xenograft specimens that contain stem cell populations alongside brain-specific perivascular niche cells in order to further understand interactions that drive cancer stem cell maintenance and therapeutic resistance. Overall, this platform will be useful for studies examining that mechanisms that govern initial associations between GBM and endothelial cells that eventually lead to invasion, as well as those that contribute to therapeutic resistance within the perivascular niche.

5. Conclusions

The perivascular niche in GBM has been implicated in contributing to tumor invasion and therapeutic resistance. Incorporating elements of the perivascular niche into 3D *in vitro* platforms is therefore instrumental in improving the usefulness of this culture system for understanding tumor biology and accurately predicting therapeutic outcome. We report that the inclusion of endothelial cells and fibroblasts in co-culture with U87-MG cells within GelMA hydrogels produces a gene expression profile that allows for further recapitulation of elements of *in vivo* GBM phenotype. Upregulation of genes related to motility and signaling alongside downregulation of genes related to cell cycle point towards a model that supports the “go or grow” phenotype. Temporal changes in gene expression additionally supported observations of endothelial network co-option and regression during the culture period. Finally, we observed enhanced resistance to the alkylating agent TMZ for GBM cells cultured in the presence of a perivascular niche in GelMA hydrogels as opposed to culture of GBM cells alone. Together, these results suggest that this platform recapitulates characteristics of native GBM behavior within the perivascular niche, and can be used to further interrogate interactions between GBM and vascular structures that contribute to tumor progression.

Acknowledgements

The authors would like to acknowledge the members of the Roy J. Carver Biotechnology Center at the University of Illinois Urbana-Champaign for their advice and assistance with experiments for this manuscript. Specifically, the authors would like to thank Drs. Barbara Pilas and Angela Kouris in the Flow Cytometry Facility, Dr. Mark Band and Tatsiana Akraiko in the Functional Genomics Unit, Dr. Alvaro Hernandez and Chris Wright in the High-Throughput Sequencing and Genotyping Unit, and Drs. Chris Fields and Jenny Zadeh in the High-Performance Biological Computing Group. The authors also gratefully acknowledge the Computer and Networking Resource Group at the Carl R. Woese Institute for Genomic Biology at the University of Illinois at Urbana-Champaign for assistance in setting up resources for high-performance computing for RNA-seq analysis. Research reported in this publication was also supported by the National Cancer Institute of the National Institutes of Health under Award Number R01 CA197488. The content is solely the responsibility of the authors and does not necessarily represent the official views of the NIH. We are grateful for the funding for this study provided by the NSF Graduate Research Fellowship DGE-1144245 (MTN). The authors are also grateful for additional funding provided by the Department of Chemical & Biomolecular Engineering and the Carl R. Woese Institute for Genomic Biology at the University of Illinois at Urbana-Champaign.

Data availability

All data analyzed during this study are included in this published article (and its supplementary information files). Raw RNA-seq data can be viewed on the NCBI GEO repository using accession number GSE111231. Other raw data required to reproduce these findings are available from the corresponding author on reasonable request.

Tables

Table 1
Taqman Gene Expression Assays used for RT-PCR.

Gene	Taqman Gene Expression Assay ID
RPS20	Hs03044413_gH
MMP9	Hs00957562_m1
TNC	Hs01115665_m1
FLT1	Hs01052961_m1
FAP	Hs00990791_m1
VEGFA	Hs00900055_m1
EGFR	Hs01076090_m1
PDGFB	Hs00966522_m1
HAS2	Hs00193435_m1
PDGFRA	Hs00998018_m1
TEK	Hs00945150_m1
PDGFRB	Hs01019589_m1
HIF1A	Hs00153153_m1
MKI67	Hs04260396_g1
RHAMM	Hs00234864_m1
HAS1	Hs00758053_m1
ANGPT1	Hs00919202_m1
ANGPT2	Hs00169867_m1

Table 2
Fraction of the cell population that is comprised of NHLFs in *Perivascular-only* and *Tri-Culture* hydrogels over the course of 14 days of culture. Data is presented as mean ± SD. N = 3.

Day	CD90+ Percentage of Total Cell Population (%)	
	Perivascular only	Tri-Culture
3	57.72 ± 2.23	51.54 ± 1.14
7	52.25 ± 3.54	32.47 ± 0.58
14	34.62 ± 7.94	13.71 ± 0.81

Supplementary Table 1
Significantly upregulated genes in *Tri-culture* RNA samples compared to *Mixed* RNA samples. Significance is determined by FDR-adjusted p-value<0.05. N = 3.

Supplementary Table 2
Significantly downregulated genes in *Tri-culture* RNA samples compared to *Mixed* RNA samples. Significance is determined by FDR-adjusted p-value<0.05. N = 3.

Supplementary Table 3
Gene Ontology (GO) terms related to biological processes that are over-represented amongst significantly upregulated genes within *Tri-culture* RNA samples compared to *Mixed* RNA samples. p<0.05 for significantly over-represented terms.

Supplementary Table 4
Gene Ontology (GO) terms related to biological processes that are over-represented amongst significantly downregulated genes within *Tri-culture* RNA samples compared to *Mixed* RNA samples. p<0.05 for significantly over-represented terms.

Supplementary Table 5
KEGG pathways that are over-represented amongst significantly upregulated genes within *Tri-culture* RNA samples compared to *Mixed* RNA samples. p<0.05 for significantly over-represented pathways.

Supplementary Table 6
KEGG pathways that are over-represented amongst significantly downregulated genes within *Tri-culture* RNA samples compared to *Mixed* RNA samples. p<0.05 for significantly over-represented pathways.

References

[1] L.M. DeAngelis, Brain tumors, N Engl J Med 344(2) (2001) 114-23.
[2] S.M. Ehsan, K.M. Welch-Reardon, M.L. Waterman, C.C. Hughes, S.C. George, A three-dimensional in vitro model of tumor cell intravasation, Integr Biol (Camb) 6(6) (2014) 603-10.
[3] I. Paw, R.C. Carpenter, K. Watabe, W. Debinski, H.W. Lo, Mechanisms regulating glioma invasion, Cancer Lett 362(1) (2015) 1-7.
[4] S. Watkins, S. Robel, I.F. Kimbrough, S.M. Robert, G. Ellis-Davies, H. Sontheimer, Disruption of astrocyte-vascular coupling and the blood-brain barrier by invading glioma cells, Nat Commun 5 (2014) 4196.
[5] K.K. Velpula, A.A. Rehman, B. Chelluboina, V.R. Dasari, C.S. Gondi, J.S. Rao, K.K. Veeravalli, Glioma stem cell invasion through regulation of the interconnected ERK, integrin alpha6 and N-cadherin signaling pathway, Cellular signalling 24(11) (2012) 2076-84.
[6] B. Ananthanarayanan, Y. Kim, S. Kumar, Elucidating the mechanobiology of malignant brain tumors using a brain matrix-mimetic hyaluronic acid hydrogel platform, Biomaterials 32(31) (2011) 7913-23.
[7] A. Clavreul, C. Guette, R. Faguer, C. Tétaud, A. Boissard, L. Lemaire, A. Rousseau, T. Avril, C. Henry, O. Coqueret, P. Menei, Glioblastoma-associated stromal cells (GASCs) from histologically normal surgical margins have a myofibroblast phenotype and angiogenic properties, J Pathol 233(1) (2014) 74-88.
[8] N.A. Charles, E.C. Holland, R. Gilbertson, R. Glass, H. Kettenmann, The brain tumor microenvironment, Glia 59(8) (2011) 1169-80.
[9] N. Charles, E.C. Holland, The perivascular niche microenvironment in brain tumor progression, Cell Cycle 9(15) (2010) 3012-21.
[10] F. Winkler, Y. Kienast, M. Fuhrmann, L. Von Baumgarten, S. Burgold, G. Mitteregger, H. Kretzschmar, J. Herms, Imaging glioma cell invasion in vivo reveals mechanisms of dissemination and peritumoral angiogenesis, Glia 57(12) (2009) 1306-15.
[11] A. Farin, S.O. Suzuki, M. Weiker, J.E. Goldman, J.N. Bruce, P. Canoll, Transplanted glioma cells migrate and proliferate on host brain vasculature: a dynamic analysis, Glia 53(8) (2006) 799-808.
[12] J. Holash, P.C. Maisonpierre, D. Compton, P. Boland, C.R. Alexander, D. Zagzag, G.D. Yancopoulos, S.J. Wiegand, Vessel cooption, regression, and growth in tumors mediated by angiopoietins and VEGF, Science 284(5422) (1999) 1994-8.
[13] D. Zagzag, R. Amirnovin, M.A. Greco, H. Yee, J. Holash, S.J. Wiegand, S. Zabski, G.D. Yancopoulos, M. Grumet, Vascular apoptosis and involution in gliomas precede neovascularization: A novel concept for glioma growth and angiogenesis, Laboratory Investigation 80(6) (2000) 837-849.
[14] A. Vartanian, S.K. Singh, S. Agnihotri, S. Jalali, K. Burrell, K.D. Aldape, G. Zadeh, GBM's multifaceted landscape: highlighting regional and microenvironmental heterogeneity, Neuro-Oncology 16(9) (2014) 1167-1175.
[15] Y. Rong, D.L. Durden, E.G. Van Meir, D.J. Brat, 'Pseudopalisading' necrosis in glioblastoma: A familiar morphologic feature that links vascular pathology, hypoxia, and angiogenesis, Journal of Neuropathology and Experimental Neurology 65(6) (2006) 529-539.
[16] M.E. Hardee, D. Zagzag, Mechanisms of glioma-associated neovascularization, Am J Pathol 181(4) (2012) 1126-41.
[17] J.D. Lathia, J.M. Heddleston, M. Venere, J.N. Rich, Deadly teamwork: neural cancer stem cells and the tumor microenvironment, Cell Stem Cell 8(5) (2011) 482-5.
[18] C. Calabrese, H. Poppleton, M. Kocak, T.L. Hogg, C. Fuller, B. Hamner, E.Y. Oh, M.W. Gaber, D. Finklestein, M. Allen, A. Frank, I.T. Bayazitov, S.S. Zakharenko, A. Gajjar, A.

Davidoff, R.J. Gilbertson, A perivascular niche for brain tumor stem cells, Cancer Cell 11(1) (2007) 69-82.
[19] N.N. Khodarev, J. Yu, E. Labay, T. Darga, C.K. Brown, H.J. Mauceri, R. Yassari, N. Gupta, R.R. Weichselbaum, Tumour-endothelium interactions in co-culture: coordinated changes of gene expression profiles and phenotypic properties of endothelial cells, J Cell Sci 116(Pt 6) (2003) 1013-22.
[20] D.T. Nguyen, Y.T. Fan, Y.M. Akay, M. Akay, Investigating Glioblastoma Angiogenesis Using A 3D in Vitro GelMA Microwell Platform, Ieee Transactions on Nanobioscience 15(3) (2016) 289-293.
[21] H.H. Song, K.M. Park, S. Gerecht, Hydrogels to model 3D in vitro microenvironment of tumor vascularization, Adv Drug Deliv Rev 79-80 (2014) 19-29.
[22] E.L. Fong, D.A. Harrington, M.C. Farach-Carson, H. Yu, Heralding a new paradigm in 3D tumor modeling, Biomaterials 108 (2016) 197-213.
[23] L. Gu, D.J. Mooney, Biomaterials and emerging anticancer therapeutics: engineering the microenvironment, Nat Rev Cancer 16(1) (2016) 56-66.
[24] C. Wang, X. Tong, F. Yang, Bioengineered 3D brain tumor model to elucidate the effects of matrix stiffness on glioblastoma cell behavior using PEG-based hydrogels, Mol Pharm 11(7) (2014) 2115-25.
[25] S.S. Rao, J. Dejesus, A.R. Short, J.J. Otero, A. Sarkar, J.O. Winter, Glioblastoma behaviors in three-dimensional collagen-hyaluronan composite hydrogels, ACS Appl Mater Interfaces 5(19) (2013) 9276-84.
[26] S.S. Rao, S. Bentil, J. DeJesus, J. Larison, A. Hissong, R. Dupaix, A. Sarkar, J.O. Winter, Inherent Interfacial Mechanical Gradients in 3D Hydrogels Influence Tumor Cell Behaviors, Plos One 7(4) (2012).
[27] S. Pedron, B.A. Harley, Impact of the biophysical features of a 3D gelatin microenvironment on glioblastoma malignancy, J Biomed Mater Res A 101(12) (2013) 3404-15.
[28] S. Pedron, E. Becka, B.A. Harley, Regulation of glioma cell phenotype in 3D matrices by hyaluronic acid, Biomaterials 34(30) (2013) 7408-17.
[29] S. Pedron, E. Becka, B.A. Harley, Spatially gradated hydrogel platform as a 3D engineered tumor microenvironment, Adv Mater 27(9) (2015) 1567-72.
[30] J.E. Chen, S. Pedron, B.A. Harley, The Combined Influence of Hydrogel Stiffness and Matrix-Bound Hyaluronic Acid Content on Glioblastoma Invasion, Macromol Biosci (2017).
[31] J.M. Heffernan, D.J. Overstreet, L.D. Le, B.L. Vernon, R.W. Sirianni, Bioengineered Scaffolds for 3D Analysis of Glioblastoma Proliferation and Invasion, Ann Biomed Eng 43(8) (2015) 1965-77.
[32] N.G. Avci, Y.T. Fan, A. Dragomir, Y.M. Akay, M. Akay, Investigating the Influence of HUVECs in the Formation of Glioblastoma Spheroids in High-Throughput Three-Dimensional Microwells, Ieee Transactions on Nanobioscience 14(7) (2015) 790-796.
[33] Z. Chen, A. Htay, W. Dos Santos, G.T. Gillies, H.L. Fillmore, M.M. Sholley, W.C. Broaddus, In vitro angiogenesis by human umbilical vein endothelial cells (HUVEC) induced by three-dimensional co-culture with glioblastoma cells, J Neurooncol 92(2) (2009) 121-8.
[34] C. Zhu, I. Chrifi, D. Mustafa, M. van der Weiden, P.J.M. Leenen, D.J. Duncker, J.M. Kros, C. Cheng, CECR1-mediated cross talk between macrophages and vascular mural cells promotes neovascularization in malignant glioma, Oncogene 36(38) (2017) 5356-5368.
[35] K. Chwalek, M.V. Tsurkan, U. Freudenberg, C. Werner, Glycosaminoglycan-based hydrogels to modulate heterocellular communication in in vitro angiogenesis models, Scientific Reports 4 (2014).
[36] L.J. Bray, M. Binner, A. Holzheu, J. Friedrichs, U. Freudenberg, D.W. Hutmacher, C. Werner, Multi-parametric hydrogels support 3D in vitro bioengineered microenvironment models of tumour angiogenesis, Biomaterials 53 (2015) 609-620.

[37] E.L.S. Fong, X.H. Wan, J. Yang, M. Morgado, A.G. Mikos, D.A. Harrington, N.M. Navone, M.C. Farach-Carson, A 3D in vitro model of patient-derived prostate cancer xenograft for controlled interrogation of in vivo tumor-stromal interactions, Biomaterials 77 (2016) 164-172.
[38] P.C. de Sampaio, D. Auslaender, D. Krubasik, A.V. Failla, J.N. Skepper, G. Murphy, W.R. English, A Heterogeneous In Vitro Three Dimensional Model of Tumour-Stroma Interactions Regulating Sprouting Angiogenesis, Plos One 7(2) (2012).
[39] F. Del Bufalo, T. Manzo, V. Hoyos, S. Yagyu, I. Caruana, J. Jacot, O. Benavides, D. Rosen, M.K. Brenner, 3D modeling of human cancer: A PEG-fibrin hydrogel system to study the role of tumor microenvironment and recapitulate the in vivo effect of oncolytic adenovirus, Biomaterials 84 (2016) 76-85.
[40] M.T. Ngo, B.A. Harley, The Influence of Hyaluronic Acid and Glioblastoma Cell Coculture on the Formation of Endothelial Cell Networks in Gelatin Hydrogels, Adv Healthc Mater 6(22) (2017).
[41] M. Wiranowska, M.V. Rojiani, Extracellular Matrix Microenvironment in Glioma Progression, in: A. Ghosh (Ed.), Glioma - Exploring its Biology and Practical Relevance, InTech2011.
[42] X. Chen, A.S. Aledia, C.M. Ghajar, C.K. Griffith, A.J. Putnam, C.C. Hughes, S.C. George, Prevascularization of a fibrin-based tissue construct accelerates the formation of functional anastomosis with host vasculature, Tissue Eng Part A 15(6) (2009) 1363-71.
[43] J.R. van Beijnum, M. Rousch, K. Castermans, E. van der Linden, A.W. Griffioen, Isolation of endothelial cells from fresh tissues, Nat Protoc 3(6) (2008) 1085-91.
[44] I.O. Vvedenskaya, S.R. Goldman, B.E. Nickels, Preparation of cDNA libraries for high-throughput RNA sequencing analysis of RNA 5' ends, Methods Mol Biol 1276 (2015) 211-28.
[45] I. Gallego Romero, A.A. Pai, J. Tung, Y. Gilad, RNA-seq: impact of RNA degradation on transcript quantification, BMC Biol 12 (2014) 42.
[46] B. Lilly, S. Kennard, Differential gene expression in a coculture model of angiogenesis reveals modulation of select pathways and a role for Notch signaling, Physiological Genomics 36(2) (2009) 69-78.
[47] S. Maekawa, A. Suzuki, S. Sugano, Y. Suzuki, RNA sequencing: from sample preparation to analysis, Methods Mol Biol 1164 (2014) 51-65.
[48] A.M. Bolger, M. Lohse, B. Usadel, Trimmomatic: a flexible trimmer for Illumina sequence data, Bioinformatics 30(15) (2014) 2114-20.
[49] A. Dobin, C.A. Davis, F. Schlesinger, J. Drenkow, C. Zaleski, S. Jha, P. Batut, M. Chaisson, T.R. Gingeras, STAR: ultrafast universal RNA-seq aligner, Bioinformatics 29(1) (2013) 15-21.
[50] Y. Liao, G.K. Smyth, W. Shi, featureCounts: an efficient general purpose program for assigning sequence reads to genomic features, Bioinformatics 30(7) (2014) 923-30.
[51] M.E. Ritchie, B. Phipson, D. Wu, Y. Hu, C.W. Law, W. Shi, G.K. Smyth, limma powers differential expression analyses for RNA-sequencing and microarray studies, Nucleic Acids Res 43(7) (2015) e47.
[52] M.D. Robinson, D.J. McCarthy, G.K. Smyth, edgeR: a Bioconductor package for differential expression analysis of digital gene expression data, Bioinformatics 26(1) (2010) 139-40.
[53] S. Falcon, R. Gentleman, Using GOstats to test gene lists for GO term association, Bioinformatics 23(2) (2007) 257-8.
[54] Y.A. Miroshnikova, J.K. Mouw, J.M. Barnes, M.W. Pickup, J.N. Lakins, Y. Kim, K. Lobo, A.I. Persson, G.F. Reis, T.R. McKnight, E.C. Holland, J.J. Phillips, V.M. Weaver, Tissue mechanics promote IDH1-dependent HIF1alpha-tenascin C feedback to regulate glioblastoma aggression, Nat Cell Biol 18(12) (2016) 1336-1345.
[55] K.J. Livak, T.D. Schmittgen, Analysis of relative gene expression data using real-time quantitative PCR and the 2(-Delta Delta C(T)) Method, Methods 25(4) (2001) 402-8.
[56] T. Hayon, A. Dvilansky, O. Shpilberg, I. Nathan, Appraisal of the MTT-based assay as a useful tool for predicting drug chemosensitivity in leukemia, Leuk Lymphoma 44(11) (2003) 1957-62.

[57] M. Hafner, M. Niepel, M. Chung, P.K. Sorger, Growth rate inhibition metrics correct for confounders in measuring sensitivity to cancer drugs, Nat Methods 13(6) (2016) 521-7.
[58] C.C. Lin, K.S. Anseth, Glucagon-like peptide-1 functionalized PEG hydrogels promote survival and function of encapsulated pancreatic beta-cells, Biomacromolecules 10(9) (2009) 2460-7.
[59] U. Verbovsek, H. Motaln, A. Rotter, N.A. Atai, K. Gruden, C.J. Van Noorden, T.T. Lah, Expression analysis of all protease genes reveals cathepsin K to be overexpressed in glioblastoma, PLoS One 9(10) (2014) e111819.
[60] G. Guo, K. Gong, S. Ali, N. Ali, S. Shallwani, K.J. Hatanpaa, E. Pan, B. Mickey, S. Burma, D.H. Wang, S. Kesari, J.N. Sarkaria, D. Zhao, A.A. Habib, A TNF-JNK-Axl-ERK signaling axis mediates primary resistance to EGFR inhibition in glioblastoma, Nat Neurosci 20(8) (2017) 1074-1084.
[61] T.E. Taylor, F.B. Furnari, W.K. Cavenee, Targeting EGFR for treatment of glioblastoma: molecular basis to overcome resistance, Curr Cancer Drug Targets 12(3) (2012) 197-209.
[62] J.R. Silber, B.A. Mueller, T.G. Ewers, M.S. Berger, Comparison of O6-methylguanine-DNA methyltransferase activity in brain tumors and adjacent normal brain, Cancer Res 53(14) (1993) 3416-20.
[63] M.C. Tate, M.K. Aghi, Biology of Angiogenesis and Invasion in Glioma, Neurotherapeutics 6(3) (2009) 447-457.
[64] J. Cha, S.G. Kang, P. Kim, Strategies of Mesenchymal Invasion of Patient-derived Brain Tumors: Microenvironmental Adaptation, Sci Rep 6 (2016) 24912.
[65] J.N. Sarkaria, G.J. Kitange, C.D. James, R. Plummer, H. Calvert, M. Weller, W. Wick, Mechanisms of chemoresistance to alkylating agents in malignant glioma, Clin Cancer Res 14(10) (2008) 2900-8.
[66] N. Charles, T. Ozawa, M. Squatrito, A.M. Bleau, C.W. Brennan, D. Hambardzumyan, E.C. Holland, Perivascular nitric oxide activates notch signaling and promotes stem-like character in PDGF-induced glioma cells, Cell Stem Cell 6(2) (2010) 141-52.
[67] K.E. Hovinga, F. Shimizu, R. Wang, G. Panagiotakos, M. Van Der Heijden, H. Moayedpardazi, A.S. Correia, D. Soulet, T. Major, J. Menon, V. Tabar, Inhibition of notch signaling in glioblastoma targets cancer stem cells via an endothelial cell intermediate, Stem Cells 28(6) (2010) 1019-29.
[68] L. Leiss, E. Mutlu, A. Oyan, T. Yan, O. Tsinkalovsky, L. Sleire, K. Petersen, M.A. Rahman, M. Johannessen, S.S. Mitra, H.K. Jacobsen, K.M. Talasila, H. Miletic, I. Jonassen, X. Li, N.H. Brons, K.H. Kalland, J. Wang, P.O. Enger, Tumour-associated glial host cells display a stem-like phenotype with a distinct gene expression profile and promote growth of GBM xenografts, BMC Cancer 17(1) (2017) 108.
[69] M.T. Ngo, B.A.C. Harley, The influence of hyaluronic acid and glioblastoma cell co-culture on the formation of endothelial cell networks in gelatin hydrogels, Advanced healthcare materials 6(21) (2017) 1700687.
[70] J.C. Gollmer, A. Ladoux, J. Gioanni, P. Paquis, A. Dubreuil, M. Chatel, C. Frelin, Expression of vascular endothelial growth factor-b in human astrocytoma, Neuro Oncol 2(2) (2000) 80-6.
[71] E. Szabo, H. Schneider, K. Seystahl, E.J. Rushing, F. Herting, K.M. Weidner, M. Weller, Autocrine VEGFR1 and VEGFR2 signaling promotes survival in human glioblastoma models in vitro and in vivo, Neuro Oncol 18(9) (2016) 1242-52.
[72] T. Ueba, J.A. Takahashi, M. Fukumoto, M. Ohta, N. Ito, Y. Oda, H. Kikuchi, M. Hatanaka, Expression of fibroblast growth factor receptor-1 in human glioma and meningioma tissues, Neurosurgery 34(2) (1994) 221-5; discussion 225-6.
[73] S.A. Raithatha, H. Muzik, H. Muzik, N.B. Rewcastle, R.N. Johnston, D.R. Edwards, P.A. Forsyth, Localization of gelatinase-A and gelatinase-B mRNA and protein in human gliomas, Neuro Oncol 2(3) (2000) 145-50.

[74] E. Serres, F. Debarbieux, F. Stanchi, L. Maggiorella, D. Grall, L. Turchi, F. Burel-Vandenbos, D. Figarella-Branger, T. Virolle, G. Rougon, E. Van Obberghen-Schilling, Fibronectin expression in glioblastomas promotes cell cohesion, collective invasion of basement membrane in vitro and orthotopic tumor growth in mice, Oncogene 33(26) (2014) 3451-3462.
[75] M. Hermanson, K. Funa, M. Hartman, L. Claesson-Welsh, C.H. Heldin, B. Westermark, M. Nister, Platelet-derived growth factor and its receptors in human glioma tissue: expression of messenger RNA and protein suggests the presence of autocrine and paracrine loops, Cancer Res 52(11) (1992) 3213-9.
[76] B. Kaur, F.W. Khwaja, E.A. Severson, S.L. Matheny, D.J. Brat, E.G. Van Meir, Hypoxia and the hypoxia-inducible-factor pathway in glioma growth and angiogenesis, Neuro Oncol 7(2) (2005) 134-53.
[77] G.P. Atkinson, S.E. Nozell, E.T. Benveniste, NF-kappaB and STAT3 signaling in glioma: targets for future therapies, Expert Rev Neurother 10(4) (2010) 575-86.
[78] H. Mao, D.G. Lebrun, J. Yang, V.F. Zhu, M. Li, Deregulated signaling pathways in glioblastoma multiforme: molecular mechanisms and therapeutic targets, Cancer Invest 30(1) (2012) 48-56.
[79] A. Giese, M.A. Loo, N. Tran, D. Haskett, S.W. Coons, M.E. Berens, Dichotomy of astrocytoma migration and proliferation, Int J Cancer 67(2) (1996) 275-82.
[80] L. Mariani, C. Beaudry, W.S. McDonough, D.B. Hoelzinger, T. Demuth, K.R. Ross, T. Berens, S.W. Coons, G. Watts, J.M. Trent, J.S. Wei, A. Giese, M.E. Berens, Glioma cell motility is associated with reduced transcription of proapoptotic and proliferation genes: a cDNA microarray analysis, J Neurooncol 53(2) (2001) 161-76.
[81] C. Charalambous, F.M. Hofman, T.C. Chen, Functional and phenotypic differences between glioblastoma multiforme-derived and normal human brain endothelial cells, J Neurosurg 102(4) (2005) 699-705.
[82] A. Stratmann, W. Risau, K.H. Plate, Cell type-specific expression of angiopoietin-1 and angiopoietin-2 suggests a role in glioblastoma angiogenesis, Am J Pathol 153(5) (1998) 1459-66.
[83] Y. Kim, S. Kumar, CD44-mediated adhesion to hyaluronic acid contributes to mechanosensing and invasive motility, Mol Cancer Res 12(10) (2014) 1416-29.
[84] S.L. Gerson, MGMT: its role in cancer aetiology and cancer therapeutics, Nat Rev Cancer 4(4) (2004) 296-307.
[85] M.E. Hegi, A.C. Diserens, T. Gorlia, M.F. Hamou, N. de Tribolet, M. Weller, J.M. Kros, J.A. Hainfellner, W. Mason, L. Mariani, J.E. Bromberg, P. Hau, R.O. Mirimanoff, J.G. Cairncross, R.C. Janzer, R. Stupp, MGMT gene silencing and benefit from temozolomide in glioblastoma, N Engl J Med 352(10) (2005) 997-1003.
[86] T. Borovski, P. Beke, O. van Tellingen, H.M. Rodermond, J.J. Verhoeff, V. Lascano, J.B. Daalhuisen, J.P. Medema, M.R. Sprick, Therapy-resistant tumor microvascular endothelial cells contribute to treatment failure in glioblastoma multiforme, Oncogene 32(12) (2013) 1539-48.
[87] J.J. Virrey, E.B. Golden, W. Sivakumar, W. Wang, L. Pen, A.H. Schonthal, F.M. Hofman, T.C. Chen, Glioma-associated endothelial cells are chemoresistant to temozolomide, J Neurooncol 95(1) (2009) 13-22.
[88] C.J. Tape, S. Ling, M. Dimitriadi, K.M. McMahon, J.D. Worboys, H.S. Leong, I.C. Norrie, C.J. Miller, G. Poulogiannis, D.A. Lauffenburger, C. Jorgensen, Oncogenic KRAS Regulates Tumor Cell Signaling via Stromal Reciprocation, Cell 165(7) (2016) 1818.
[89] S. Darmanis, S.A. Sloan, D. Croote, M. Mignardi, S. Chernikova, P. Samghababi, Y. Zhang, N. Neff, M. Kowarsky, C. Caneda, G. Li, S.D. Chang, I.D. Connolly, Y. Li, B.A. Barres, M.H. Gephart, S.R. Quake, Single-Cell RNA-Seq Analysis of Infiltrating Neoplastic Cells at the Migrating Front of Human Glioblastoma, Cell Rep 21(5) (2017) 1399-1410.
[90] A.P. Patel, I. Tirosh, J.J. Trombetta, A.K. Shalek, S.M. Gillespie, H. Wakimoto, D.P. Cahill, B.V. Nahed, W.T. Curry, R.L. Martuza, D.N. Louis, O. Rozenblatt-Rosen, M.L. Suva, A. Regev,

B.E. Bernstein, Single-cell RNA-seq highlights intratumoral heterogeneity in primary glioblastoma, Science 344(6190) (2014) 1396-401.
[91] S. Pedron, H. Polishetty, A.M. Pritchard, B.P. Mahadik, J.N. Sarkaria, B.A.C. Harley, Spatially-graded hydrogels for preclinical testing of glioblastoma anticancer therapeutics, MRS Commun 7(3) (2017) 442-449.